Supplementary Information

Differential effects of MoO_3 and MoO_2 sacrificial layer on J-V performance of $Cu_2ZnSn(S, Se)_4$ solar cells

Jinhui Zhang, [†a] Chuanhe Ma, [†a] Haixuan Gao[a], Jinchun Jiang[b] and Hailong Wang[*a]

[a]*School of Physics and Physical Engineering, Qufu Normal University, Qufu 273165, China.*

[b]*Key Laboratory of Polar Materials and Devices (MOE), Department of Electronic science, East China Normal University, Shanghai 200241, China*

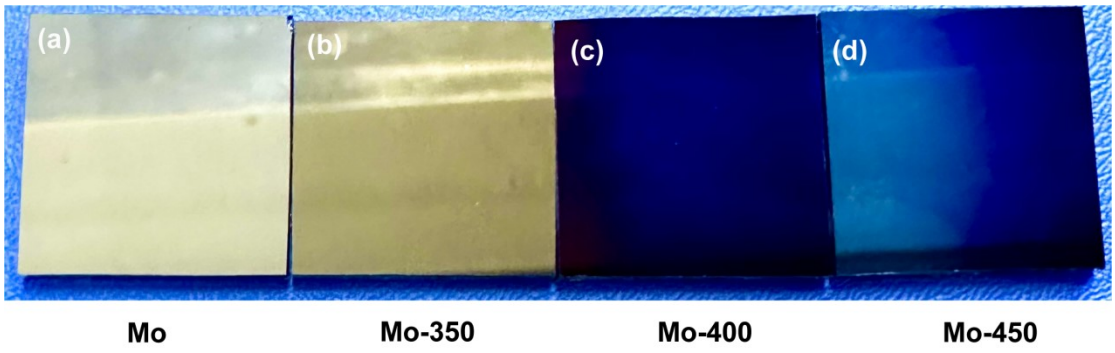

Figure S1. *The macroscopic morphology of Mo substrate after oxidation annealing in air at different temperatures: (a) without annealing; (b) 350 ℃; (c) 400 ℃; (d) 450 ℃.*

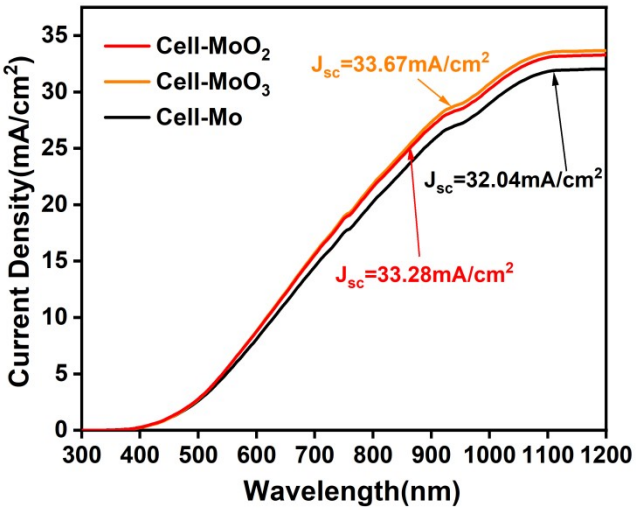

Figure S2. *Integrated current density (J_{int}) of different solar cell devices that fit based on AM1.5G spectral: Cell-Mo, Cell-MoO_3, Cell-MoO_2.*

* Corresponding author; E-mail: hlwang@qfnu.edu.cn, Fax: +86 0537-4456092.

†First author: they contribute to this work equally.

Based on the AM1.5G spectrum, we fitted different solar cell devices' integrated current density (J_{int}), as shown in Figure S2. The J_{SC} values of Cell Mo, Cell-MoO_3, and Cell-MoO_2 calculated based on the EQE spectrum are 32.04 mA/cm^2, 33.28 mA/cm^2, and 33.67 mA/cm^2, respectively, which is consistent with the J_{SC} obtained from the J-V curves. This indicates that the main reason for improving PCE by the sacrificial layer of MoO_3 is to increase J_{sc}.

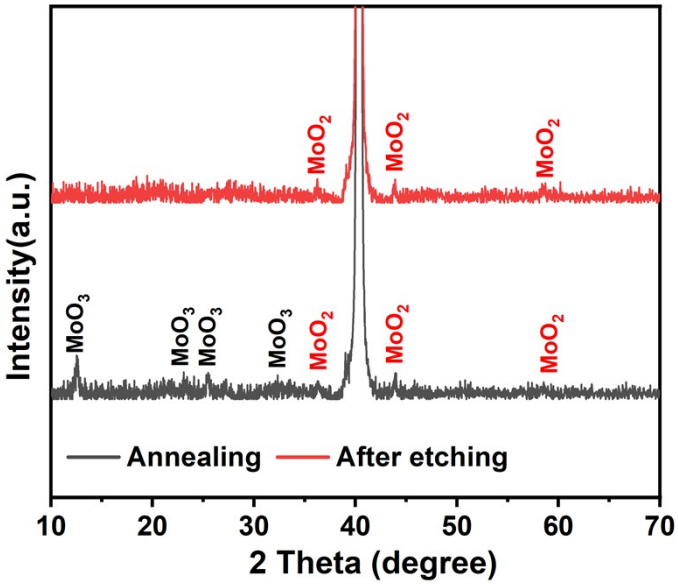

Figure S3. *XRD patterns of Mo substrate by oxidation annealing at 450℃ and after ammonia etching.*

To observe the characteristic peaks related to MoO_2 and MoO_3, we increased the oxidation annealing temperature from 350 ℃ to 450 ℃ to increase the thickness of the sacrificial layer and tested its XRD and Raman characteristics. As shown in Figure S3, the samples annealed at 450 ℃ exhibit XRD peaks related to MoO_3 at 12.5°, 23°, 25.4°, and 32.3°, and XRD peaks related to MoO_2 at 36.2°, 43.9°, and 58.4°. After ammonia etching, the XRD peaks related to MoO_3 disappear, leaving only the XRD peaks related to MoO_2.

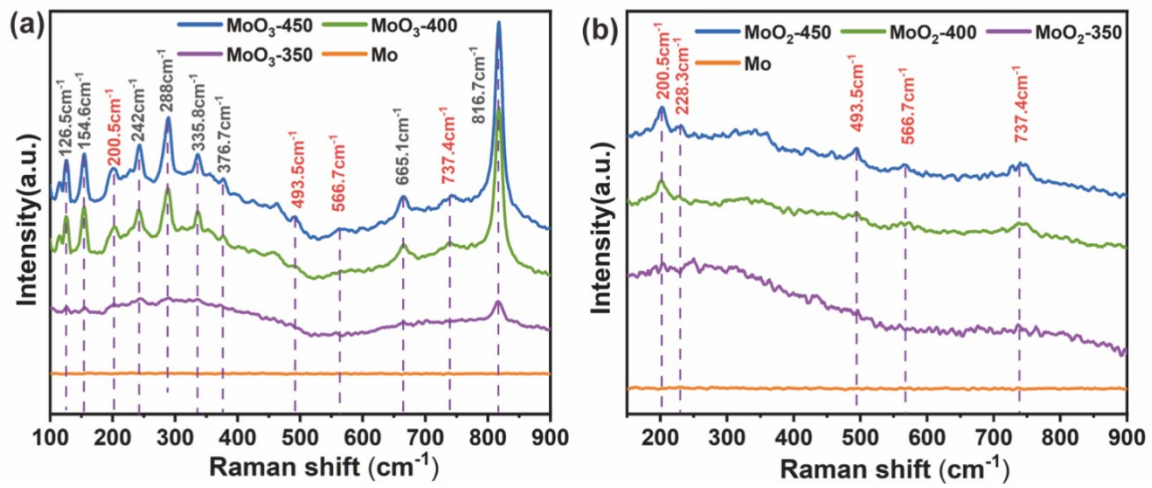

Figure S4. *(a) Raman spectra of Mo substrates after increasing the oxidation annealing temperature to 350 ℃, 400 ℃, and 450 ℃; (b) Raman spectra of the corresponding Mo substrates after ammonia etching.*

In addition, we also investigated the effects of 450 ℃ oxidation annealing and ammonia etching on the Raman characteristic peaks related to MoO_2 and MoO_3. As shown in Figure S4, the samples annealed at 450 ℃ exhibit Raman peaks associated with MoO_3 at 126.5cm^{-1}, 154.6cm^{-1}, 242cm^{-1}, 288cm^{-1}, 335.8cm^{-1}, 376.7cm^{-1}, and 665.1cm^{-1}, and Raman peaks associated with MoO_2 at 200.5cm^{-1}, 228.3cm^{-1}, 493.5cm^{-1}, 566.7cm^{-1} and 737.4cm^{-1}. After ammonia etching, the Raman peaks associated with MoO_3 disappear, leaving only the Raman peaks related to MoO_2.

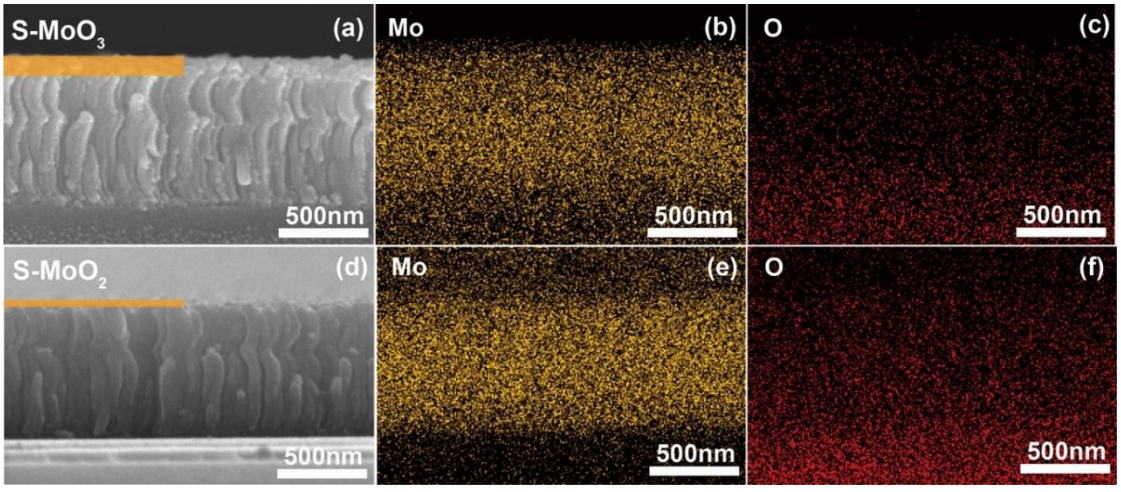

Figure S5. *Cross-sectional SEM images and EDX element mappings of the substrate with MoO_3 (a-c) and substrate with MoO_2 (d-f). For the EDX element mappings, the color of the Mo element is golden, and the O element is red.*

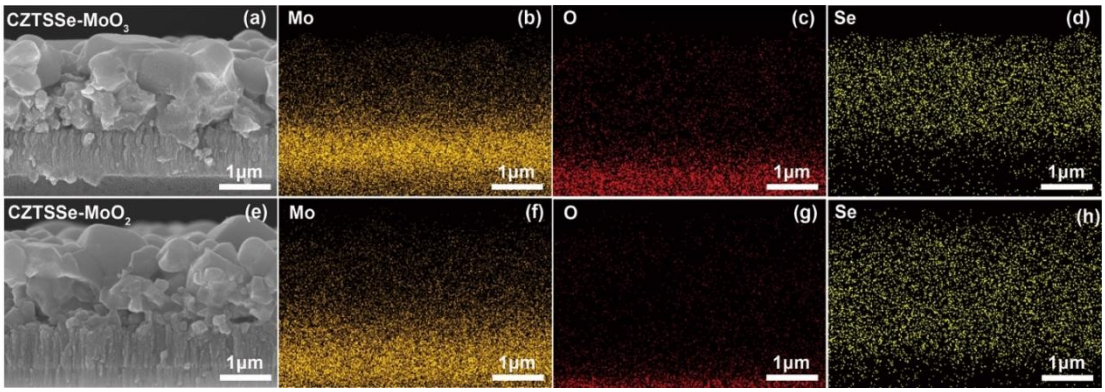

Figure S6. *Cross-sectional SEM images and EDX element mappings of selenized CZTSSe films on MoO_3 (a-d) and MoO_2 (e-h) substrates. For the EDX element mappings, the color of the Mo element is golden, the O element is red, and the Se element is yellow.*

Figure S5 shows the SEM cross-sectional and EDX element mappings of the substrate with MoO_3 sacrificial layer (Fig. 5(a)-(c)) prepared by direct oxidation annealing at 350℃ and substrate with MoO_2 sacrificial layer (Fig. 5(d)-(f)) after ammonia etching, respectively. Figure S6 shows the cross-sectional SEM images and EDX element mappings of the CZTSSe films after selenide annealing of MoO_3 substrate (Fig. 6(a)-(d)) and MoO_2 substrate (Fig. 6(e)-(h). For the EDX element mappings, the color of the Mo element is golden, the O element is red, and the Se element is yellow. The EDX element mapping shows that the O element (Figs. S5(c), S5(f)) diffuses into the Mo substrate after oxidation annealing. In contrast, the O signal in the substrate is significantly weakened after selenide annealing (Figs. S6(c), S6(g)). Se signals are enhanced at the location of the layers of MoO_3 (Fig. S6(d)) and MoO_2 (Fig. S6(h)), which proves that the MoO_x layers transform into $MoSe_2$ layer after selenide annealing.

By comparing Figure S5 and S6, we can draw the following two conclusions. Firstly, selenide annealing weakens the oxygen signal within the substrate, while the selenium signal becomes stronger. This explains the meaning of the sacrificial layer, which means that MoO_x can only partially (not wholly) block the diffusion of Se elements into the Mo substrate, and MoO_x will eventually be replaced by $MoSe_2$. Secondly, the blocking effect of the MoO_3 sacrificial layer is better than that of the MoO_2 sacrificial layer, which can be demonstrated by

the thinner thickness of the $MoSe_2$ layer in Figure S6 (d) compared to Figure S6 (h).